Scientia Iranica, Vol. 13, No. 3, pp 272–283

SCIENTIA IRANICA

Dynamics Modeling of "CEDRA" Rescue Robot on Uneven Terrain

A. Meghdari*, S.H. Mahboobi[1] and A. Lotfi Gaskarimahalle[2]

This paper presents an effective approach for kinematic and dynamic modeling of high mobility Wheeled Mobile Robots (WMR). As an example of these robots, the method has been applied to the CEDRA rescue robot, which is a complex, multibody mechanism. The model is derived for 6-DOF motions, enabling movements in x, y and z directions, as well as for roll, pitch and yaw rotations. Forward kinematics equations are derived using the Denavit-Hartenberg method and Jacobian matrices for the wheels. Moreover, the inverse kinematics of the robot are obtained and solved for the wheel velocities and steering commands, in terms of the desired velocity, heading and measured link angles. Finally, the dynamics of the rover mechanism have been thoroughly studied and analyzed. Due to the complexity of this multi-body system, especially on rough terrain, Kane's method of dynamics has been used to model this problem. The proposed approach and method can easily be extended to other mechanisms and rovers.

INTRODUCTION

Rescue operations and future outer space explorations will require high mobility robots to perform intricate tasks in challenging uneven terrain. In order to avoid the presence of humans in unknown and hazardous environments, from collapsed construction after an earthquake to inspections on alien planets, autonomous applications seem to be mandatory. Current motion planning and control algorithms are not well suited to rough terrain mobility. In fact, trajectory tracking is mostly concentrated on planar motion, since it does not generally consider the physical characteristics of the rover and its environment.

Although lots of researchers have dealt with the case of flat surfaces, they have rarely considered dynamic analysis for rough terrain and most of the recent research in outdoor operations has discussed just simple mechanisms. One of the earliest works on the formulation of WMRs kinematics equations of motion has been studied by Muir et al. [1]. They extended the methodology to accommodate special characteristics of WMRs, such as multiple closed-loop chains, higher-pair contact points between a wheel and a surface and unactuated and unsensed wheel Degrees Of Freedom (DOF). One of the valuable parts of the survey, utilized in this paper, was the interpretation of the properties of a composite robot equation to guarantee their existence and to characterize the mobility of a WMR, according to the mobility characterization tree.

Kinematic studies of six-wheel rocker-bogie rovers, such as JPL Sojourner rover, have been presented in [2] and [3]. Tarokh et al. [4] have conducted research on the direct and inverse kinematics of Rocky7 using the Denavit-Hartenberg algorithm. Although it presented a relatively complete kinematics model, terrain unevenness, which causes slippage and all of the angular variations, has been ignored.

Also, dynamic modeling of a wheeled mobile robot with suspension has been considered in [5]. Although the approach is novel, no exact dynamic equation has been derived from this research, thus, it cannot be implemented on the control unit. Generally, no one has presented a closed form dynamic equation for a multi-wheeled rover without simplifying the problem.

In this paper, an effective approach for kinematic and dynamic modeling of high mobility Wheeled Mobile Robots (WMR) has been presented. As an example of these robots, the method has been applied to the CEDRA rescue robot, which is a complex, multibody mechanism [6] (Figure 1). The CEDRA rescue robot is one of several laboratory robots made

*. *Corresponding Author, Department of Mechanical Engineering, Sharif University of Technology, Tehran, I.R. Iran.*

1. *Department of Mechanical Engineering, Sharif University of Technology, Tehran, I.R. Iran.*
2. *Department of Mechanical Engineering, Pennsylvania State University, Pennsylvania, USA.*

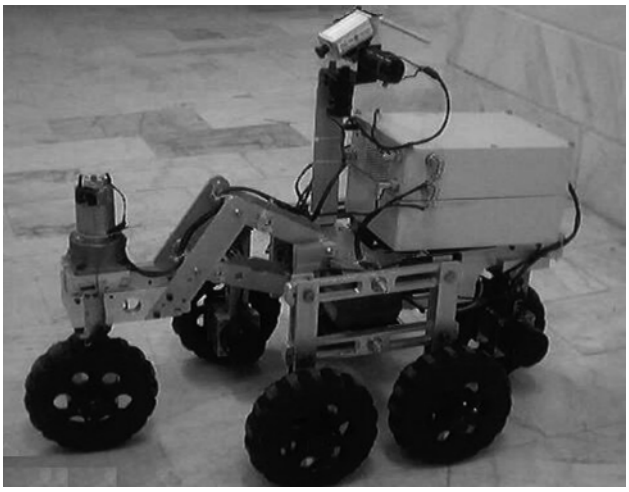

Figure 1. CEDRA rescue robot.

at the Center of Excellence in Design, Robotics and Automation (CEDRA).

The main structure of this robot is based on a shrimp-like mechanism, developed in EPFL [7], consisting of three main parts (see Figure 2): Main body, parallel bogies and front fork (a four-link mechanism):

1. *Body*: The main part of the robot, as a container for electronic boards, batteries, camera, navigation and victim detection instruments;
2. *Parallel Bogies*: This consists of two parallel four-link mechanisms mounted on each side of the main body, in order to stabilize it and increase the terrain adaptability of the robot;
3. *Front Fork*: A four-link mechanism mounted in front of the robot body that helps the robot in climbing obstacles.

Using a D-H coordinate definition, the forward kinematics of the system have been evaluated in terms of joint angles and wheel rotations. Then, the parameters are separated, according to the actuated and sensed parameters, leading to the inverse kinematics of the rover.

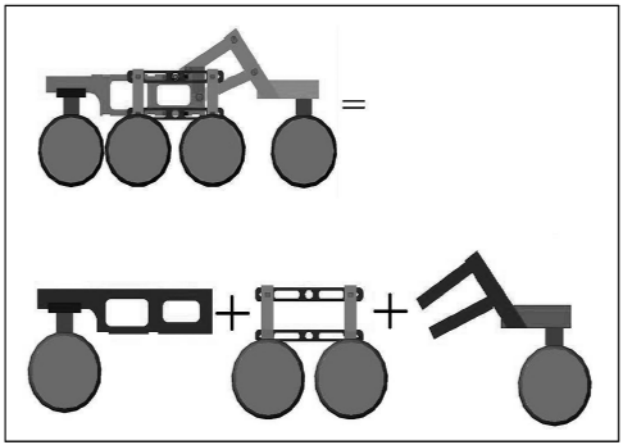

Figure 2. Three main parts of a shrimp mechanism.

Another demanding objective is to model the complicated dynamics of the CEDRA robot for use on uneven terrain. Since the robot is a 6-wheel rover with 2 steering commands and many linkages, Kane's approach has been preferred to other methods. Considering really rough terrain modeling, the flexibility of the tire and ground interaction has also been considered in the dynamic model.

KINEMATIC MODELING

The first step in the modeling of robots is kinematic modeling. In this analysis, the motion of mass center will be determined in terms of known wheel motions and vice versa. Also, by setting a desired velocity for the mass center, one can derive the actuators velocity so that it can be utilized in the kinematic based control of the system.

The approach that will be discussed here is the basis for a kinematic analysis of WMRs on uneven terrain. At first, a frame-work is constructed to express the position-orientation of the desired points, like wheel centers, contact points and joints. All these coordinates are defined using the Denavit-Hartenberg (D-H) method [8]. Then, by evaluating the transformation matrices between the robot reference frame and each wheel motion frame, the relative position of the motion frame, with respect to the robot center of mass, is derived. In order to obtain the robot forward kinematic, Jacobian matrices for each wheel are evaluated in a symbolic manner.

Coordinate Definition

All the coordinate frames used in this article are right-hand coordinate systems. The robot reference frame is defined at the center of mass so that the x direction refers to forward motion and the z-axis heads upward. According to the D-H method [8], a coordinate frame is introduced on each joint. Since CEDRA is a 6-wheel robot, there are 6 separate open chains. Figures 3 and 4 depict the robot coordination.

A transformation matrix can be defined between two consequent frames, using the D-H parameters, a_i, α_i, d_i, θ_i:

$$ {}^{i-1}T_i = \begin{bmatrix} c\theta_i & s\theta_i c\alpha_i & s\theta_i s\alpha_i & a_i c\theta_i \\ s\theta_i & c\theta_i c\alpha_i & c\theta_i s\alpha_i & a_i s\theta_i \\ 0 & s\alpha_{i-1} & c\alpha_{i-1} & d_i \\ 0 & 0 & 0 & 1 \end{bmatrix}, \qquad (1) $$

where:

$$ \begin{aligned} c\theta_i &= \cos\theta_i, & s\theta_i &= \sin\theta_i, \\ c\alpha_{i-1} &= \cos\alpha_{i-1}, & s\alpha_{i-1} &= \sin\alpha_{i-1}. \end{aligned} \qquad (2) $$

Table 1 provides the D-H parameters corresponding to the coordinate frames in Figures 3 and 4.

Then, by cascading the transformation matrices in the chains, the position of each wheel is obtained in the body coordinate, named the robot reference frame. In fact, the transformation matrices are the augmented matrix of a 3×3 rotation matrix and a 3×1 translation (position) vector.

For example, for the transformation from the rover reference frame, R, to the wheel 1 axle frame, one has the following:

$$^{R}T_1 = {}^{R}T_{Bl}\,{}^{Bl}T_1. \tag{3}$$

However, in order to capture the wheel motion, one needs two more coordinate frames. Two additional coordinate frames are defined for each wheel, i.e., contact frame C_i and motion frame M_i, $i = 1,\cdots,6$. The contact coordinate frame, C_i, defines the location of the wheel-terrain contact point. It is obtained by a rotation of the wheel axle coordinate frame about the z-axis, followed by a 90 degree rotation about the x-axis. The z-axis of the C_i frame points away from the contact point, as illustrated in Figure 5. The D-H parameters for the C_i frames, $i = 1,\cdots,6$, are provided in Table 2.

The wheel motion frame, M_i, accounts for the wheel roll and rotational slip. It is obtained by rotating about the C_i frame's z-axis a rotational slip (ξ_i), translating along the negative z-axis by the wheel radius (R_w) and, finally, translating along the x-axis for wheel roll ($R_w.\gamma_i$) on a virtual inclined surface, as illustrated in Figure 5. Corresponding D-H parameters are provided in Table 3.

Now, one can write the transformation matrices for each wheel's motion coordinate frame (M_i), in

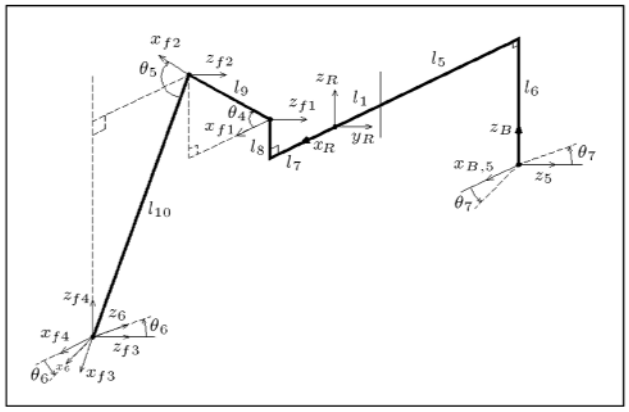

Figure 3. Body and front fork coordinates.

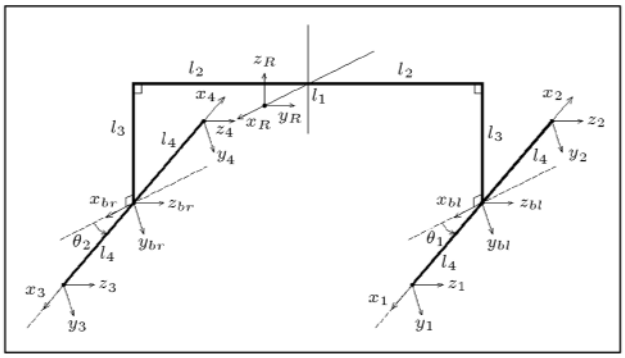

Figure 4. Bogie coordinates.

Table 1. D-H parameters for wheel center coordinate frames.

Frame	a_i	α_i	d_i	θ_i
B_l	l_1	$\pi/2$	l_3	0
B_r	l_1	$\pi/2$	l_3	0
B	l_1 l_5	0	l_6	0
F_1	l_1	0	l_8	0
F_2	l_1	$\pi/2$	0	θ_4
F_3	l_1	0	0	θ_5
F_4	0	$\pi/2$	0	θ_4 θ_5
Wheel#1	l_4	0	0	θ_1
Wheel #2	l_4	0	0	$\pi+\theta_1$
Wheel #3	l_4	0	0	θ_2
Wheel #4	l_4	0	0	$\pi+\theta_2$
Wheel #5	0	$\pi/2$	0	θ_3
Wheel #6	0	$\pi/2$	0	θ_6

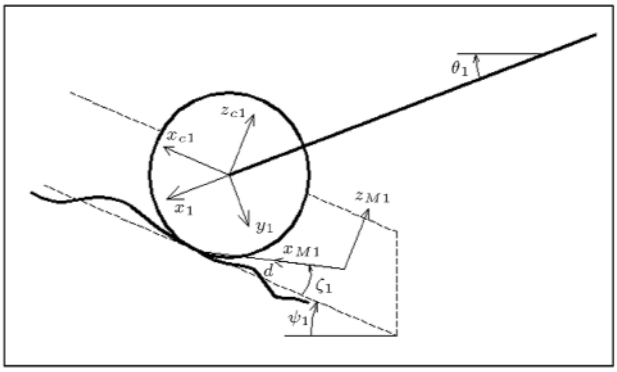

Figure 5. Contact and motion frames.

Table 2. D-H parameters for contact coordinate frames.

Frame	a_i	α_i	d_i	θ_i
C_1	0	$\pi/2$	0	θ_1 Ψ_1
C_2	0	$\pi/2$	0	π θ_1 Ψ_2
C_3	0	$\pi/2$	0	θ_2 Ψ_3
C_4	0	$\pi/2$	0	π θ_2 Ψ_4
C_5	0	$\pi/2$	0	Ψ_5
C_6	0	$\pi/2$	0	Ψ_6

Table 3. D-H parameters for motion coordinate frames.

Frame	a_i	α_i	d_i	θ_i
M_1	$R_w.\gamma_1$	0	R_w	ξ_1
M_2	$R_w.\gamma_2$	0	R_w	ξ_2
M_3	$R_w.\gamma_3$	0	R_w	ξ_3
M_4	$R_w.\gamma_4$	0	R_w	ξ_4
M_5	$R_w.\gamma_5$	0	R_w	ξ_5
M_6	$R_w.\gamma_6$	0	R_w	ξ_6

terms of the rover's reference frame (R). The transformations for wheel 1 are as follows:

$$^{R}T_{M1} = ^{R}T_{Bl}\,^{Bl}T_{1}\,^{1}T_{C1}\,^{C1}T_{M1}. \tag{4}$$

Forward Kinematics

In view of the fact that the inverse of the transformation matrix is equal to the inverse chain transformation matrix, one has the following [4]:

$$^{R}\dot{T}_{R} = ^{R}T_{M_i}\,^{M_i}\dot{T}_{R}. \tag{5}$$

In contrast with Tarokh et al. [4] who have substituted $\gamma_i = 0$, the absolute rotations of the wheels, γ_i, will disappear from these equations, meaning that there should not be any angular position in the velocity distribution. Tarokh et al. [4] have substituted $\theta_i = 0$, but, in fact, there should not be any angular position in the velocity distribution.

Using $Z \quad Y \quad X$ Euler angles, ϕ (heading), p (pitch) and r (roll), the derivative of the rover coordinate frame, $^{R}\dot{T}_{R}$, is found to have the following form:

$$^{R}\dot{T}_{R} = \begin{bmatrix} 0 & \dot{\phi} & \dot{p} & \dot{x} \\ \dot{\phi} & 0 & \dot{r} & \dot{y} \\ \dot{p} & \dot{r} & 0 & \dot{z} \\ 0 & 0 & 0 & 1 \end{bmatrix}. \tag{6}$$

The angles correspond to rotations about the rover's reference frame (i.e., ϕ about the z-axis, p about the y-axis and r about the x-axis).

After factorization of the velocity components of joint angles in the right side of Equation 5 and extracting the velocity vector, $v = \begin{bmatrix} \dot{x} & \dot{y} & \dot{z} & \dot{\phi} & \dot{p} & \dot{r} \end{bmatrix}^T$, the Jacobian matrix for each wheel is derived as follows:

$$v = J_i \dot{q}_i \qquad i = 1, \cdots, 6. \tag{7}$$

For instance, for wheel 1, one has the following:

$$v = \begin{bmatrix} l_4 s(\theta_1) & R_w c(\psi_1) c(\xi_1) & l_2 c(\psi_1) + l_3 c(\psi_1) & l_3 + l_4 s(\theta_1) \\ 0 & R_w s(\xi_1) & l_1 c(\psi_1) + l_4 c(\theta_1 + \psi_1) & 0 \\ l_4 c(\theta_1) & R_w s(\psi_1) c(\xi_1) & l_2 s(\psi_1) & l_1 + l_4 c s(\theta_1) \\ 0 & 0 & c(\psi_1) & 0 \\ 0 & 0 & 0 & 1 \\ 0 & 0 & s(\psi_1) & 0 \end{bmatrix} \begin{bmatrix} \dot{\theta}_1 \\ \dot{\gamma}_1 \\ \dot{\xi}_1 \\ \dot{\psi}_1 \end{bmatrix}. \tag{8}$$

Inverse Kinematics

The actuated inverse solution is used by solving Equation 7 for the actuated wheel velocities. The outputs of the trajectory tracking controller are generally the rover forward velocity and turning rate. So, $\dot{x}_d$ and $\dot{\phi}_d$ are introduced as the controller commands. Also, bogie angles $\dot{\theta}_1$ and $\dot{\theta}_2$ and front four-link angle $\dot{\theta}_4$ can be measured relative to the body. It is assumed that the path planning unit has provided a complete sense of the terrain profile ($Z = f(X, Y)$) and one has $\dot{\psi}_1 (i = 1..6)$ at the contact points. Moreover, the outputs of the inverse kinematics unit should be the angular velocity of the actuators, consisting of 6 wheel motors and 2 steering motors.

Because of the closed-link chains in the wheeled mobile robot, it is not necessary to actuate all of the wheel variables. To separate the actuated and unactuated wheel variables, the wheel kinematic equation is partitioned into two components, as follows [1]:

$$E_i v_d = J_{ai} \dot{q}_{ai} + J_{ui} \dot{q}_{ui}, \qquad i = 1, \cdots, 6. \tag{9}$$

As an example for the 1st wheel, one has the following:

$$\begin{bmatrix} 1 & 0 & l_4 s(\theta_1) & l_3 & l_4 s(\theta_1) \\ 0 & 0 & 0 & & 0 \\ 0 & 0 & l_4 c(\theta_1) & l_1 & l_4 c(\theta_1) \\ 0 & 1 & 0 & & 0 \\ 0 & 0 & 0 & & 1 \\ 0 & 0 & 0 & & 0 \end{bmatrix} \begin{bmatrix} \dot{x}_d \\ \dot{\phi}_d \\ \dot{\theta}_1 \\ \dot{\psi}_1 \end{bmatrix}$$

$$= \begin{bmatrix} R_w c(\psi_1) c(\xi_1) \\ R_w s(\xi_1) \\ R_w s(\psi_1) c(\xi_1) \\ 0 \\ 0 \\ 0 \end{bmatrix} \dot{\gamma}_1$$

$$+\begin{bmatrix} & l_2c(\psi_1) & 0 & 0 & 0 & 0 \\ l_3s(\psi_1) & l_1c(\psi_1)+l_4c(\theta_1+\psi_1) & 1 & 0 & 0 & 0 \\ & l_2s(\psi_1) & 0 & 1 & 0 & 0 \\ & c(\psi_1) & 0 & 0 & 0 & 0 \\ & 0 & 0 & 0 & 1 & 0 \\ & s(\psi_1) & 0 & 0 & 0 & 1 \end{bmatrix}$$

$$\begin{bmatrix} \dot{\xi}_1 \\ \dot{y} \\ \dot{z} \\ \dot{p} \\ \dot{r} \end{bmatrix}, \tag{10}$$

where the left side refers to the controller commands and the known parameters, J_{ai} is the Jacobian of actuated components and J_{ui} is the Jacobian of unactuated components.

Then, the actuated inverse solution is applied in [1], as follows:

$$\dot{q}_{ai} = \left[J_{ai}^T \Delta(J_{ui}) J_{ai}\right]^{-1} J_{ai}^T \Delta(J_{ui}) E_i v_d, \quad i = 1, \cdots, 6, \tag{11}$$

where:

$$\Delta(J) = J(J^T J)^{-1} J^T - I. \tag{12}$$

By substituting and simplifying the above equations, the following is obtained:

$$\dot{\gamma}_1 = \frac{\dot{x}_d - l_2\dot{\phi}_d - l_4\sin(\theta_1)\dot{\theta}_1 - (l_3 + l_4\sin(\theta_1))\dot{\psi}_1}{R_w\cos(\psi_1)\cos(\xi_1)},$$

$$\dot{\gamma}_2 = \frac{\dot{x}_d - l_2\dot{\phi}_d + l_4\sin(\theta_1)\dot{\theta}_1 - (l_3 - l_4\sin(\theta_1))\dot{\psi}_2}{R_w\cos(\psi_2)\cos(\xi_2)},$$

$$\dot{\gamma}_3 = \frac{\dot{x}_d + l_2\dot{\phi}_d - l_4\sin(\theta_2)\dot{\theta}_2 - (l_3 + l_4\sin(\theta_2))\dot{\psi}_3}{R_w\cos(\psi_3)\cos(\xi_3)},$$

$$\dot{\gamma}_4 = \frac{\dot{x}_d + l_2\dot{\phi}_d + l_4\sin(\theta_2)\dot{\theta}_2 - (l_3 - l_4\sin(\theta_2))\dot{\psi}_4}{R_w\cos(\psi_4)\cos(\xi_4)},$$

$$\dot{\gamma}_5 = \frac{\dot{x}_d - l_6\cos(\theta_3)\dot{\psi}_5}{R_w(\cos(\theta_3)\cos(\psi_5)\cos(\xi_5) - \sin(\theta_3)\sin(\xi_5))},$$

$$\dot{\gamma}_6 = \frac{\dot{x}_d + l_8\dot{\theta}_4 - (l_8 + l_9\sin(\theta_4))\dot{\theta}_5}{R_w(\sin(\theta_4+\theta_5+\theta_6)\sin(\xi_6)+\cos(\theta_4+\theta_5+\theta_6)\cos(\psi_6)\cos(\xi_6))}. \tag{13}$$

As can be seen, the steering rate cannot be derived through this method, since it is coupled with the rotational slip.

Geometric Method for Steering Angles

Since steering and rotational slip cannot be distinguished for steerable wheels, one cannot use the Jacobian approach for steering commands as is used for the wheel rotation velocities. Therefore, a geometric approach is used, which determines the desired instantaneous steering angle.

Due to the fact that the 4 bogie wheels are nonsteerable, rotational slip plays an important role in the direction of the wheel center velocity during robot turning and each fixed wheel determines the instantaneous turn center, as illustrated in Figure 6.

First, $R_w\dot{\gamma}_1$ and $\dot{\xi}_1$ components are rewritten for fixed wheels, such as wheel 1:

$$\dot{x}_1 = R_w\dot{\gamma}_1 = \frac{\dot{x}_d - l_2\dot{\phi}_d - l_4\sin(\theta_1)\dot{\theta}_1 - (l_3 + l_4\sin(\theta_1))\dot{\psi}_1}{\cos(\psi_1)}, \tag{14}$$

$$\dot{\phi}_1 = \dot{\xi}_1 = \frac{\dot{\phi}_d}{\cos(\psi_1)}. \tag{15}$$

Each non-steerable wheel independently determines an instantaneous turn radius and turn center location [4]:

$$r_i = \frac{\dot{x}_i}{\dot{\phi}_i}, \tag{16}$$

$$c_{\text{turn}_i} = {}^R T_{Ci} r_i \vec{y}_{Ci}, \qquad i = 1, \cdots, 4. \tag{17}$$

For wheel 1, one obtains the following:

$$r_1 = \frac{\dot{x}_d - l_2\dot{\phi}_d - l_4\sin(\theta_1)\dot{\theta}_1 - (l_3 + l_4\sin(\theta_1))\dot{\psi}_1}{\dot{\phi}_d}, \tag{18}$$

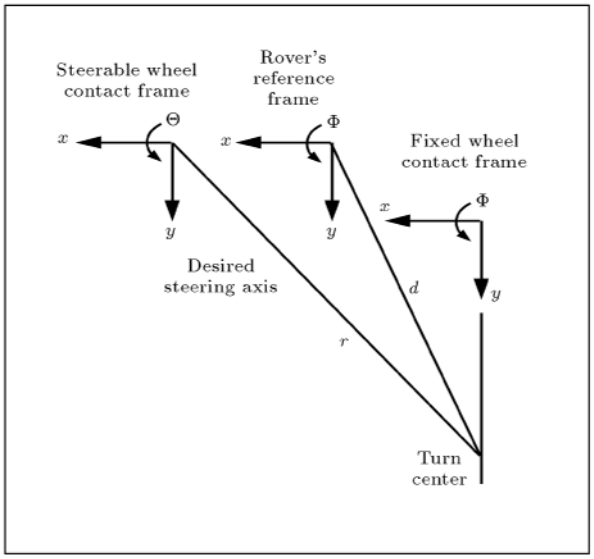

Figure 6. Coordinate frames for steering angle calculations.

$$c_{\text{turn}_1} = {}^R T_{C1} r_1 \vec{y}_{C1}$$

$$= \begin{bmatrix} c(\psi_1) & 0 & s(\psi_1) & l_1 + l_4 c(\theta_1) \\ 0 & 1 & 0 & l_2 \\ s(\psi_1) & 0 & c(\psi_1) & l_3 \quad l_4 s(\theta_1) \\ 0 & 0 & 0 & 1 \end{bmatrix} \begin{bmatrix} 0 \\ r_1 \\ 0 \\ 1 \end{bmatrix}$$

$$= \begin{bmatrix} l_1 + l_4 \cos(\theta_1) \\ \frac{\dot{x}_d \quad l_2 \dot{\phi}_d \quad l_4 s(\theta_1)\dot{\theta}_1 \quad (l_3 + l_4 s(\theta_1))\dot{\psi}_1}{\dot{\phi}_d} + l_2 \\ l_3 \quad l_4 s(\theta_1) \\ 1 \end{bmatrix}. \quad (19)$$

Here, there are four unique turn centers, which will be unified by an approximation method [4]:

$$c_{\text{turn}_R} = \frac{1}{4} \sum_{i=1}^{4} c_{\text{turn}_i}. \quad (20)$$

Now, using a geometric approach, the steering angles will be found (see Figure 6). The vector, r, defines the turn center relative to the steering wheel contact coordinate frame. Then, this quantity is determined for each steerable wheel, as follows [4]:

$$r_i = {}^R T_{Ci}^{\,1} c_{\text{turn}_R}, \qquad i = 5, 6, \quad (21)$$

where, c_{turn_R} is the estimated turn center calculated in the previous section and ${}^R T_{Ci}$ is the transformation matrix between the rover's reference frame and the wheel, i, contact frame. Since the steerable axis is the z-axis, one is only concerned with the projection of r in the $x \quad y$ plane.

The desired steering angle for steerable wheel i is, then;

$$\theta_i = a \tan 2 \left(\quad \text{sign}(r_{yi}) r_{xi}, |r_{yi}| \right), \qquad i = 5, 6. \quad (22)$$

KANE'S METHOD

Kane's method, developed in the 1980's, is the most recent approach to motion dynamic analysis [9]. This method has demonstrated conspicuous predominance over others, like Newton and Lagrange, in complex problems. In fact, the efficacy of this approach is related to the lower number of equations, closed forms of equations, ease of deriving the constraint forces and better implementation of the numerical solutions, especially in dealing with the multiplicity of masses in the system. It is also widely used in nonholonomic problems, since the Lagrange method cannot handle nonholonomic constraints easily.

Kane's method uses the same list of definitions for its concepts as the Newtonian method, but, in order to distinguish the new expressions, a word "generalized" appears as a prefix to that concept. For a system with n-Degrees Of Freedom (DOF) and m-generalized coordinates, "generalized speeds" are defined as follows:

$$u_r = z_r(q,t) + \sum_{i=1}^{m} y_{ri}(q,t)\dot{q}_1, \qquad (1 < r < n), \quad (23)$$

where $\dot{q}_i$ is the time derivative of q and y_{ri} and z_r are functions of q and time t. The word "speed" is to show the scalar nature of the parameter.

The number of generalized speeds is equal to the number of DOF. According to the definition of generalized speed and by solving the equation for $\dot{q}_i$, one has the following:

$$\dot{q}_s = Z_s(q,t) + \sum_{i=1}^{n} Y_{si}(q,t)\dot{u}_i, \qquad (1 < s < m), \quad (24)$$

where, Z_s and Y_{si} are functions of q and time t.

Now, the partial linear velocity and the partial angular velocity of point P are introduced, as follows:

$$\vec{V}_r^{\,P} = \frac{\partial \vec{V}^P}{\partial u_r}, \quad (25)$$

$$\vec{\omega}_r^{\,B} = \frac{\partial \vec{\omega}^B}{\partial u_r}, \quad (26)$$

V^P and ω^B are the velocities of point P. Also, the velocity of any point can be derived from the linear combination of partial velocities associated with that point:

$$\vec{V}^P = \vec{v}^P(q,t) + \sum_{i=1}^{n} \vec{V}_i^{\,P} u_i, \quad (27)$$

$$\vec{\omega}^B = \vec{W}^B(q,t) + \sum_{i=1}^{n} \vec{\omega}_i^B u_i. \quad (28)$$

Like other methods based on the calculus of variation (such as the Lagrange method), here, the generalized forces are defined, which means the partial derivative of active forces or torques inserting energy to the system. These forces might be external or internal, like internal friction forces.

$$F_r = \sum_{i=1}^{\lambda} \vec{V}_r^{\,i} . \vec{R}^i + \sum_{j=1}^{\gamma} \vec{\omega}_r^{\,j} . \vec{M}^j, \quad (29)$$

$\vec{R}^i$ $(1 \le i \le \lambda)$ is for λ active forces and $\vec{M}^j$ $(1 \le j \le \gamma)$ is for γ active torques. In this approach, inertial terms are considered, due to the D'Alambert viewpoint of dynamic equations, and can be written as follows:

$$\vec{\tilde{R}}^B = \quad m_B \vec{a}^B, \quad (30)$$

$$\vec{\tilde{M}}^B = \quad (I^B \vec{\alpha}^B + \vec{\omega}^B \times I^B \vec{\omega}^B). \quad (31)$$

By summation of these equations for all bodies, one obtains the following:

$$F_r^* = \sum_{i=1}^{\beta} \left(\vec{V}_r^i . \widetilde{\vec{R}}^i + \vec{\omega}_r^i . \widetilde{\vec{M}}^i \right). \tag{32}$$

Equilibrium equations associated with the D'Alambert viewpoint will lead to Kane's equations and can be represented as:

$$F_r^* + F_r = 0. \tag{33}$$

Kinematic Constraints

To get a better sense of the dynamic problem, the Degrees Of Freedom (DOF) and the required parameters for a determined configuration are discussed.

Consider the main body in 3D space with 6 DOF. Adding 3 angular freedoms in the bogies and front fork, 6 wheel rotations and 2 steering angles allow the rover to have 17 DOF in space. But, since it traverses on the ground, 6 motions will be confined and the total number of DOF will equal 11. In the condition of no longitudinal slip, 6 other DOF will be limited and the total DOF decreases to 5.

Here, a complete model of rover motion is to be developed, in which slipping and skidding (i.e., longitudinal and transversal slippage) will be considered.

To determine the robot configuration completely, 11 independent parameters should be assigned, which are chosen here to be $\dot{x}$, $\dot{y}$, $\dot{\phi}$, $\dot{\gamma}_{1..6}$, $\dot{\theta}_3$ and $\dot{\theta}_6$ (steering), as generalized speeds.

In order to find the ground reaction force, a velocity is introduced at the center of each wheel. Therefore, the normal force and total friction force on the wheels can be derived.

Finally, the total number of generalized coordinates equals 35 and their rate of change will be:

$$\dot{q} = \Big[\underbrace{\dot{\theta}_{1,2}}_{\text{Bogie}} \quad \underbrace{\dot{\theta}_4}_{\text{Fork}} \quad \dot{z} \quad \dot{p} \quad \dot{r} \quad \underbrace{V_{wx}}_{6} \quad \underbrace{V_{wy}}_{6} \quad \underbrace{V_{wz}}_{6} \quad \dot{x} \quad \dot{y} \quad \dot{\phi} \quad \underbrace{\dot{\gamma}_i}_{6} \quad \underbrace{\dot{\theta}_{3,6}}_{\text{Steering}} \Big]^T. \tag{34}$$

Since the normal velocity of wheel centers relative to the ground is a virtual velocity, an additional set of generalized speeds is defined. If the terrain profile is defined as $Z = f(X, Y)$, one will have the following:

$$u_j = \begin{bmatrix} V_{w_i x} \\ V_{w_i y} \\ V_{w_i z} \end{bmatrix} . \nabla f, \quad \text{for}: \ j = 12 \cdots 17. \tag{35}$$

As mentioned above, one needs to find 18 constraints to confine 35 generalized coordinates to 17 generalized speeds. Figure 7 illustrates the schematic 2D sketch of closed loop chains between the rover reference frame and wheels. The other bogie has not been shown here, so, there are six 3D constraints. $\dot{\theta}_5$ has been omitted from the generalized coordinates, hence, the relation between $\dot{\theta}_4$ and $\dot{\theta}_5$ in the front fork is not considered in the constraints.

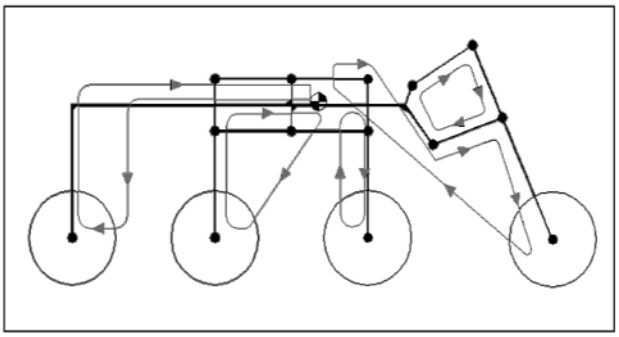

Figure 7. Closed-loop chains.

In the kinematic part, the velocities of the wheel centers have been defined in the rover reference frame, R, using the D-H method described in the previous sections. For example, for wheel 1, one has a closed loop chain as follows:

$$V_{w1} \quad \left[I_{3\times 3} \ \vdots \ 0_{3\times 1} \right] {}^{o}T_R \, {}^{R}T_{w1} \left[0 \quad 0 \quad 0 \quad 1 \right]^T = 0, \tag{36}$$

in which, ${}^{o}T_R$ is the transformation matrix of the robot reference frame, with respect to the global coordinate.

$${}^{o}T_R = \begin{bmatrix} c(\phi)c(p) & c(\phi)s(p)s(r) & c(\phi)s(p)c(r) & x \\ & s(\phi)c(r) & +s(\phi)c(r) & \\ s(\phi)c(p) & s(\phi)s(p)s(r) & s(\phi)s(p)c(r) & y \\ & +c(\phi)c(r) & c(\phi)s(r) & \\ s(p) & c(p)s(r) & c(p)c(r) & z \\ 0 & 0 & 0 & 1 \end{bmatrix}. \tag{37}$$

Since Equation 36 presents 3 motion constraints, 18 constraint equations will be obtained by the closed-loop chains.

Now, the constraint equations need to be rearranged to construct a standard form of Equation 24. For this purpose, the generalized coordinates are factorized and, then, the definition of inputs are augmented, leading to a 35×35 matrix.

$$\begin{bmatrix} A_{18\times 35} \\ \cdots\cdots\cdots\cdots \\ 0_{17\times 18} \ \vdots \ I_{17\times 17} \end{bmatrix} \dot{q}_{35\times 1} = \begin{bmatrix} 0_{1\times 18} \ \vdots \ u_1 \ u_2 \ \cdots \ u_{17} \end{bmatrix}, \tag{38}$$

or:

$$A_{1(35\times 35)}(q)\dot{q} = \sum_{i=1}^{17} B_i u_i,$$

where:

$$B_i^T = \left[0_{1\times(17+i)} \quad \vdots \quad 1 \quad \vdots \quad 0_{1\times(17\ \ i)}\right], \tag{39}$$

or:

$$\dot{q} = A_1{}^1(q)\sum_{i=1}^{17} B_i u_i = \sum_{i=1}^{17} G_{i(35\times1)}\, u_i.$$

DYNAMICAL ANALYSIS

In this section, a systematic procedure for the dynamic modeling and formulation of WMRs is presented for 3D motion on rough terrain. The analysis will be based on Kane's method. Here, an approach for extraction of Kane's items, like generalized inertial forces and generalized active forces, has been demonstrated. As an illustrative example, this method has been applied to the CEDRA rescue robot.

Inertial Forces

Since a distributed mass analysis is very demanding and does not seem to be reasonable in rover dynamics, 8 noticeable point masses are assumed consisting of 6 wheels, a front fork and a main body. The velocities of these masses will easily be evaluated using the D-H method explained in the previous section.

$$V^{wj} = \left[I_{3\times3} \quad \vdots \quad 0_{3\times1}\right] {}^oT_R\, {}^RT_{wj} \left[0 \quad 0 \quad 0 \quad 1\right]^T,$$

$$\text{for } j = 1..6, \tag{40}$$

$$V^{FF} = \left[I_{3\times3} \vdots 0_{3\times1}\right] {}^oT_R\, {}^RT_{f4} \left[x_{FF} \quad 0 \quad z_{FF} \quad 1\right]^T, \tag{41}$$

$$V^{MB} = \left[I_{3\times3} \vdots 0_{3\times1}\right] {}^oT_R\, {}^RT_{MB} \left[x_{MB} \ 0 \ z_{MB} \ 1\right]^T, \tag{42}$$

or:

$$V^{mj} = \widetilde{V}^{mj}_{3\times35}(q)\dot{q}_{35\times1} = \sum_{i=1}^{17}\left[\widetilde{V}^{mj}_{3\times35} G_{i(35\times1)}\right] u_i,$$

$$\text{for } j = 1..8. \tag{43}$$

The partial velocities of the wheel centers can be expressed as:

$$\vec{V}_r^{\,p} = \frac{\partial \vec{V}^p}{\partial u_r} \Rightarrow \vec{V}_r^{\,mj} = [\widetilde{V}^{mj}_{3\times35} G_{r(35\times1)}]. \tag{44}$$

Also, accelerations associated with point masses are found by the derivation of velocities, as follows:

$$\begin{aligned} a^{mj} &= \frac{d}{dt}V^{mj} \\ &= \sum_{i=1}^{17}\left\{\left[\widetilde{V}^{mj}_{3\times35} G_{i(35\times1)}\right]\dot{u}_i + \frac{\partial[\widetilde{V}^{mj}_{3\times35} G_{i(35\times1)}]}{\partial q}\dot{q}u_i\right\} \\ &= \sum_{i=1}^{17}[\widetilde{V}^{mj} G_i]\dot{u}_i + \sum_{i=1}^{17}\sum_{k=1}^{17}\left[\frac{\partial[\widetilde{V}^{mj} G_i]}{\partial q} G_k\right] u_k u_i. \end{aligned} \tag{45}$$

Furthermore, one needs to evaluate the angular velocity vectors of the wheels, the main body and the front fork:

$$\omega^{wj} = {}^oT^{\text{rotation}}_{R(3\times3)}\left(\begin{bmatrix}\dot{r}\\ \dot{p}\\ \dot{\phi}\end{bmatrix} + \begin{bmatrix}0\\ \dot{\gamma}_j\\ 0\end{bmatrix}\right), \quad \text{for } j = 1..6, \tag{46}$$

$$\omega^{FF} = {}^oT^{\text{rotation}}_{R(3\times3)}\left(\begin{bmatrix}\dot{r}\\ \dot{p}\\ \dot{\phi}\end{bmatrix} + \begin{bmatrix}0 & \\ \dot{\theta}_4 & \dot{\theta}_5\\ 0 & \end{bmatrix}\right), \tag{47}$$

$$\omega^{MB} = {}^oT^{\text{rotation}}_{R(3\times3)}\begin{bmatrix}\dot{r}\\ \dot{p}\\ \dot{\phi}\end{bmatrix}, \tag{48}$$

or:

$$\omega^{mj} = \widetilde{\omega}^{mj}_{3\times35}(q)\dot{q}_{35\times1} = \sum_{i=1}^{17}\left[\widetilde{\omega}^{mj}_{3\times35} G_{i(35\times1)}\right] u_i,$$

$$\text{for } j = 1..8, \tag{49}$$

where ${}^oT^{\text{rotation}}_{R(3\times3)}$ is the rotational part of ${}^oT_R$ and the corresponding partial angular velocity will be:

$$\vec{\omega}_r^{\,mj} = [\widetilde{\omega}^{mj}_{3\times35} G_{r(35\times1)}], \tag{50}$$

$$\begin{aligned} \alpha^{mj} &= \frac{d}{dt}\omega^{mj} = \sum_{i=1}^{17}[\widetilde{\omega}^{mj} G_i]\dot{u}_i \\ &\quad + \sum_{i=1}^{17}\sum_{k=1}^{17}\left[\frac{\partial[\widetilde{\omega}^{mj} G_i]}{\partial q} G_k\right] u_k u_i. \end{aligned} \tag{51}$$

The generalized forces are derived by substituting the above parameters in Equations 30 to 32.

$$F_1^* = \sum_{j=1}^{8}\left(m_j(\vec{V}_1^{\,mj}.\vec{a}^{mj}) + I_j(\omega_1^{mj}\alpha^{mj})\right). \tag{52}$$

Gravity Force

The partial velocities associated with each weight force exertion point are equal to the partial velocities of the center of gravity of the bodies. Also, the weight forces are simply described by:

$$\vec{F}^{w_j} = \quad m_j g \begin{bmatrix} 0 \\ 0 \\ 1 \end{bmatrix}. \tag{53}$$

Motor Torques

Inserted energy to the system is provided by the motors; hence, the torque vector is defined as:

$$\tau = \begin{bmatrix} \tau_1 & \tau_2 & \tau_3 & \tau_4 & \tau_5 & \tau_6 \end{bmatrix}^T, \tag{54}$$

and the angular velocities of these torques are:

$$\omega^{\tau_j} = \dot{\phi}_j \quad \dot{\psi}, \qquad j = 1,\ 2,\ 3,\ 4,\ 5,$$

$$\omega^{\tau_6} = \dot{\phi}_6 \quad \dot{\beta}. \tag{55}$$

Now, by defining E in the form of:

$$E_r = \begin{bmatrix} \widetilde{\omega}^{\tau_1} & \widetilde{\omega}^{\tau_2} & \widetilde{\omega}^{\tau_3} & \widetilde{\omega}^{\tau_4} & \widetilde{\omega}^{\tau_5} & \widetilde{\omega}^{\tau_6} \end{bmatrix} TG_r, \tag{56}$$

the motor torques in dynamics modeling can be included.

Ground Force

An interaction force is exerted under each wheel that can be defined as:

$$F^{gj} = \begin{bmatrix} F_x^{gj} \\ F_y^{gj} \\ F_z^{gj} \end{bmatrix}. \tag{57}$$

The velocity of the ground force action point is easily evaluated using the motion coordinate frame, after setting ξ to zero.

$$V^{cj} = \begin{bmatrix} I_{3\times 3} & \vdots & 0_{3\times 1} \end{bmatrix} {}^{o}T_R {}^{R}T_{mj} \begin{bmatrix} 0 & 0 & 0 & 1 \end{bmatrix}^T$$

$$= \begin{bmatrix} V_x^{cj} \\ V_y^{cj} \\ V_z^{cj} \end{bmatrix}_{3\times 1} = \begin{bmatrix} \widetilde{V}_x^{cj} \\ \widetilde{V}_y^{cj} \\ \widetilde{V}_z^{cj} \end{bmatrix} \dot{q} = \sum_{i=1}^{17} \left(\begin{bmatrix} \widetilde{V}_x^{cj} \\ \widetilde{V}_y^{cj} \\ \widetilde{V}_z^{cj} \end{bmatrix} G_i \right) u,$$

$$\text{for } j = 1..6, \tag{58}$$

$$V_r^{cj} = \begin{bmatrix} \widetilde{V}_x^{cj} \\ \widetilde{V}_y^{cj} \\ \widetilde{V}_z^{cj} \end{bmatrix} G_r. \tag{59}$$

And, eventually, the generalized force associated with the contact points is:

$$F_r^g = \sum_{j=1}^{6} V_r^{cj} . \vec{F}^{gj} \tag{60}$$

Kane Formulation

The closed form equation for the dynamics of the rover can be derived as follows:

$$\sum_{i=1}^{17} M_{r_i}(q)\dot{u}_i + \sum_{i=1}^{17}\sum_{j=1}^{17} N_{r_{i,j}}(q) u_i u_j + gW_r(q)$$

$$+ F_r^g(q, \vec{F}^{gj}) = \tau . E_r(q), \qquad r = 1..17, \tag{61}$$

where the coefficients are:

$$M_r(q) = \sum_{j=1}^{8} (m_j [\widetilde{V}^{C_j} A_1 {}^1] . [\widetilde{V}^{C_j} A_1 {}^1]$$

$$+ I_j [\widetilde{\omega}^j A_1 {}^1] . [\widetilde{\omega}^j A_1 {}^1]),$$

$$N_r(q) = \sum_{j=1}^{8} (m_j [\widetilde{V}^{C_j} A_1 {}^1] . \frac{\partial [\widetilde{V}^{C_j} A_1 {}^1]}{\partial q}$$

$$+ I_j [\widetilde{\omega}^j A_1 {}^1] . \frac{\partial [\widetilde{\omega}^j A_1 {}^1]}{\partial q}) A_1 {}^1,$$

$$W_r(q) = \sum_{j=1}^{8} m_j [\widetilde{V}^{C_j} A_1 {}^1] . \begin{bmatrix} 0 \\ 0 \\ 1 \end{bmatrix}. \tag{62}$$

The above equations are the closed form equations of motion for the CEDRA rover, consisting of 17 equations, 17 generalized speeds and 18 ground force components. Hence, one should find 18 constraint equations. The dynamics of WMRs, in the presence of slip, do not usually have an analytical solution, since in non-slip conditions, a kinematic constraint restricts the rotational motion of the wheel and, in cases of slipping, a dynamic constraint relates the normal force with the friction force. Therefore, a decision tree is needed for the numerical solution. First, a rigid wheel on a rigid terrain is considered:

(I) Wheel j doesn't slip:

(1) Because of skidding, transversal friction force is equal to:

$${}^{C}F_y^{gj} = \quad \mu_s {}^{C}F_z^{gj}, \tag{63}$$

where, ${}^{C}F_z^{gj}$ and ${}^{C}F_y^{gj}$ are the normal and transversal ground reaction forces in the contact coordinate frame;

(2) It is assumed that wheels do not lose their contacts, so,

$$u_{12} = u_{13} = \cdots = u_{17} = 0. \tag{64}$$

(3) The longitudinal motion of each wheel is dependant on the wheel rotation.

$$V_{xj} = R_w \dot{\gamma}_j, \qquad j = 1..6, \tag{65}$$

where the longitudinal velocity is the projection of V^{wj} in the contact frame x-axis direction.

With these 18(= 3 × 6) extra constraints, they can be solved simultaneously with Equation 61. At each time step, 35 equations with 35 unknowns are solved and all ground contact forces are determined. Now, assumption I should be checked for validity.

$$\frac{\sqrt{({}^C F_x^{gj})^2 + ({}^C F_y^{gj})^2}}{{}^C F_z^{gj}} \leq \mu_s. \tag{66}$$

If Condition 66 doesn't hold for the obtained forces, this time step should be solved once again with assumption II.

(II) Wheel j slips:

(1) Friction force that is always in the direction of motion is, as follows:

$$\frac{V_{xj}}{V_{yj}} = \frac{{}^C F_x^{gj}}{{}^C F_y^{gj}}. \tag{67}$$

(2) Equation 64 is valid for this case too;

(3) The dynamic constraint of contact force is:

$$\sqrt{({}^C F_x^{gj})^2 + ({}^C F_y^{gj})^2} = \mu_s^C F_z^{gj}. \tag{68}$$

Again, after solving 35 equations, one goes through the next time step. Now, in a more realistic approach, the ground flexibility in the constraints is considered. The method does not change, except for the assumptions made in the previous section. Since the friction coefficient changes its nature, Equation 63 does not hold in this case.

SIMULATION

The obtained equations can be used for various purposes, such as: Dynamics optimization, checking available control strategies, inverse and forward dynamic simulation and comparison between various rovers. But, as far as there has been a focus on obtaining the equations themselves, only a simpler simulation is described. Due to the complexity of the 3D case, the simulation illustrated here will concentrate on the 2D vertical plane. There are several reasons for this 2D simulation. The mechanisms (like bogies and front fork) move in parallel planes and there is no linkage and flexibility in the 3rd dimension. Therefore, the rover dimensions are more effective and more meaningful in the planner analysis. Moreover, the first step in the design of rovers is checking its capability of climbing over obstacles and this model has been used to develop climbing abilities through dynamical equations of motion. In simulation, the robot is forced to pass a bump generated by a function like "$he^{(\frac{x}{w})^2}$", similar to the previous work [10]. The "h" is selected equal to "w" and about 2.25 times the wheel radius. It is assumed that all six wheels torques are equal. The above mentioned task has been applied to the robot and the results are shown in Figure 8. As can be seen, after a transient response, it will follow the same behavior as before. Consequently, the values of normal forces, friction forces and their ratios have changed.

CONCLUSIONS

A general frame-work for kinematic and dynamic analysis of rovers has been developed, consisting of forward and inverse kinematics in a control oriented approach and by deriving the dynamics equations based on Kane's method. The analysis has been applied to the CEDRA rescue robot as an illustrating example. In order to reach a desired velocity on rough terrain, the equations of the actuators' effort have been derived.

This work has mainly focused on the detailed steps of dynamic formulation rather than dynamic analysis of the CEDRA robot. However, future work is required to perform a more exact analysis of this robot and to extend the application of this method.

Based on D-H and Kane's methods, a systematic method for deriving equations of motion governing a rover has been presented. The method is very efficient for numerical purposes.

In addition, it has been shown that the method is capable of extracting exact symbolic equations for a rover with one of the most complicated mechanisms, including four closed chains. Also, it is capable of calculating constraint forces easily and handling them to generate traction control algorithms for high velocities over uneven terrain. Both the kinematics and kinetics are presented here and, also, this method offers an appropriate set of coordinates to fully and easily describe rover configuration. This method, which can be used in the selection of state variables, extraction of rate equations and, also, in meaningful descriptions of various terms of equations, is very useful and novel in its own right. It must be mentioned that for 3-dimensional motion, governing equations are highly complicated and seem not to be handled and solved symbolically. Hence, a numerical method may be used to deal with the problem.

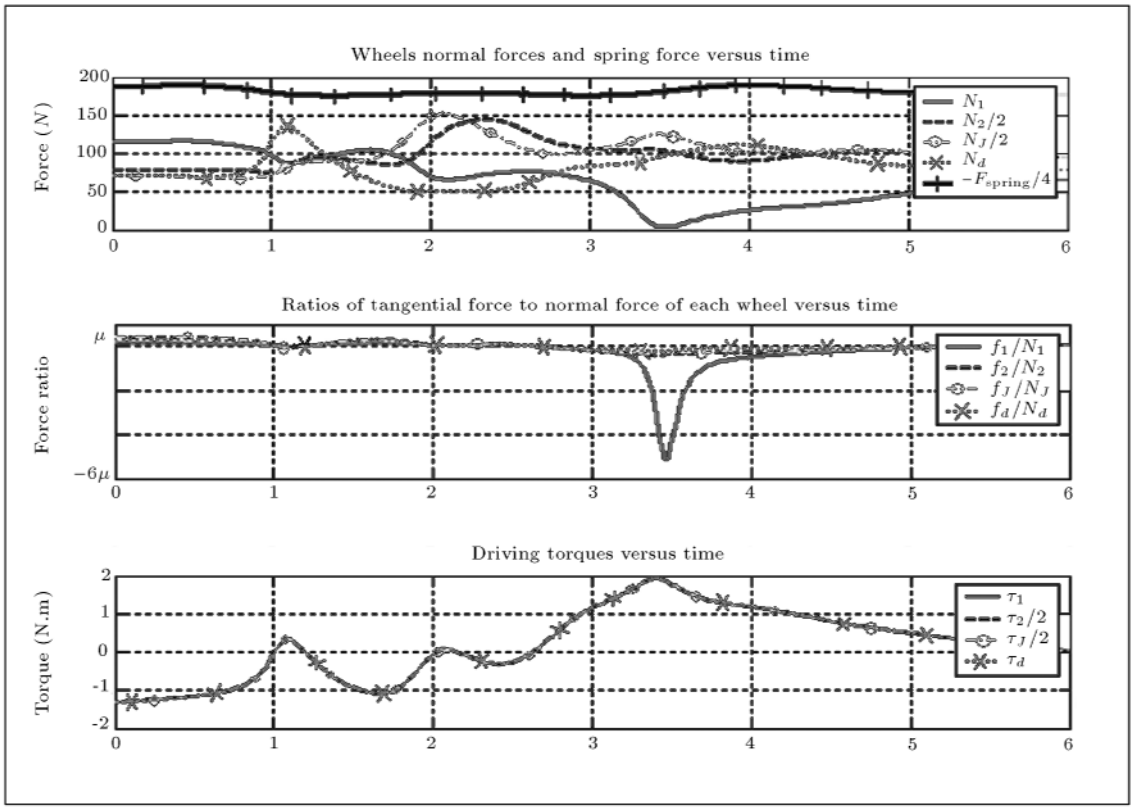

Figure 8. Simulation results for ground forces and motor torques vs. time.

NOMENCLATURE

${}^{B}T_{A}$	transformation matrix from A to B
a_i, α_i and d_i	joint parameters in D-H notation
θ_i	joint variable in D-H notation
B_l	left bogie coordinate frame
B_r	right bogie coordinate frame
B	back coordinate frame
F_i	ith front coordinate frame
C_i	ith contact coordinate frame
M_i	ith motion coordinate frame
R_w	wheel radius
ψ_i	ground slope under ith wheel
γ_i	ith wheel absolute rotation
ξ_i	angular slip
$\dot{x}, \dot{y}, \dot{z}$	robot velocities in direction of body coordinate frame
Φ, r, p	robot yaw, roll and pitch angles
$\dot{x}_d$	desired longitudinal velocity
v	velocity vector
J	Jacobian matrix
q_i	ith wheel parameter vector
J_{ai}	ith wheel actuated Jacobian matrix
J_{ui}	ith wheel unactuated Jacobian matrix
q_{ai}	ith wheel actuated parameter vector
q_{ui}	ith wheel unactuated parameter vector
c_i	instantaneous turn center for ith unsteerable wheel
r_i	turn radius for ith unsteerable wheel
F_r	sum of generalized non-inertia forces
u	generalized speeds column vector
$\dot{q}$	rate of change of generalized coordinates
g	gravitational acceleration
N	wheel normal force column vector
$\dot{\phi}_d$	desired yaw rate
c_{turn_R}	instantaneous robot turn center
m_j	mass of jth part
$\vec{V}_r^{mj}$	rth partial mass center velocity of jth part
$\vec{\omega}_r^{mj}$	rth partial mass center angular velocity of jth part
$\vec{V}^{mj}$	mass center velocity of jth part
$\vec{\omega}^{mj}$	mass center angular velocity of jth part
$\vec{a}^{mj}$	mass center acceleration of jth part

$\vec{\alpha}^{mj}$	mass center angular acceleration of jth part
I^B	moment of inertia of body B around the CM
F_r^*	sum of generalized inertia forces
τ	wheels torque column vector
$\underset{\sim}{\omega}^{\tau_i}$	corresponding angular velocity to ith applied torque
$\dot{u}$	rate of change of generalized speeds
$F_x^{gj}, F_y^{gj}, F_z^{gj}$	components of ground reaction in global coordinate frame
${}^C F_x^{gj}, {}^C F_y^{gj}, {}^C F_z^{gj}$	components of ground reaction force in the contact coordinate frame

REFERENCES

1. Muir, P.F. and Neuman, C.P. "Kinematic modeling of wheeled mobile robots", *J. Robotics Systems*, **4**(2), pp 281-340 (1987).
2. Chottiner, J.E. "Simulation of a six-wheeled martain rover called the rocker-bogie", M.S. Thesis, Ohio State University, Columbus, Ohio, USA (1992).
3. Linderman, R. and Eisen, H. "Mobility analysis, simulation and scale model testing for the design of wheeled planetary rovers", In *Missions Technologies and Design of Planetary Mobile Vehicle*, Toulouse, France, pp 531-537 (1992).
4. Tarokh, M., McDermott, G., Hayati, S. and Hung, J. "Kinematic modeling of a high mobility Mars rover", *IEEE Conf. on Robotics and Automation*, Detroit, MI, (May 1999).
5. Tai, M. "Modeling of wheeled mobile robot on rough terrain", *ASME International Mechanical Engineering Congress*, Washington, D.C., USA (2003).
6. Meghdari, A., Pishkenari, H.N., Gaskarimahalle, A.L., Mahboobi, S.H. and Karimi, R. "Optimal design and fabrication of CEDRA rescue robot using genetic algorithm", *CD-ROM Proceeding of the ASME-DETC-2004 (MR-57190)*, Salt Lake City, Utah (2004).
7. Siegwart, R., Lamon, P., Estier, T., Lauria, M. and Piguet, R. "Innovative design for wheeled locomotion in rough terrain", *J. of Robotics and Autonomous Systems*, **40**(3), pp 151-162 (2002).
8. Craig, J.J., *Introduction to Robotics: Mechanics and Control*, 2nd Ed., Addison-Wesley Pub., USA (1989).
9. Kane, T.R. and Levinson, D.A., *Dynamics: Theory and Applications*, McGraw-Hill (1985).
10. Meghdari, A., Karimi, R., Pishkenari, H.L., Gaskarimahalle, A.L. and Mahboobi, S.H. "An effective approach for dynamic analysis of rovers", *Robotica*, **23**(6), pp 771-780 (2005).